



Tono basin climate modeling, the potential advantage of fully coupled WRF/WRF-Hydro modeling System

Edward Naabil¹ · Kouakou Kouadio² · Benjamin Lamptey³ · Thompson Annor⁴ · Ifeanyi Chukwudi Achugbu⁵

Received: 18 August 2022 / Accepted: 13 October 2022 / Published online: 31 October 2022
© The Author(s), under exclusive licence to Springer Nature Switzerland AG 2022

Abstract

The climate and hydrological cycle are influenced by the relationships between land-surface characteristics and the atmosphere. According to this research, a hydrological–atmospheric coupled model adds value to river basin climate modeling by determining if it is useful. The Tono basin in Ghana's Ghana was the focus of the research, which looked at the climate of West Africa as a whole. Simulations of WRF and WRF-Hydro (WRF/WRF-Hydro) were conducted separately and together. Both runs use the same physical parameterizations. There were two methods used to evaluate the model's ability to predict precipitation and temperature in the basin: statistical analysis and spatial bias analysis. The coupled model outperformed the uncoupled model in terms of precipitation and temperature prediction. Coupling models can be used to simulate sub-grid hydrological basin features, like the Tono irrigation dam, as a result of this study.

Keywords Coupled model · WRF · WRF-Hydro · River basin · Climate

Introduction

Socioeconomic activities around the world, particularly in West Africa, have always been threatened by droughts and floods (W.A). It is becoming more commonplace in the Sahelian part of West Africa (Sylla et al. 2015). For these reasons, an irrigation project was developed in the Tono basin to lessen the effects of drought, increase crop production, and thus provide food security and raise the income levels of rural people. On the other hand, the drought's negative effects continue to have an impact on the socioeconomic activities of the basin's surrounding population. Low rainfall in 2014 meant that the dam's storage level was at its lowest point ever (a level of 173.6 amls). Irrigation farming in the basin was put on hold, resulting in the loss of livelihoods for 6,000 farmers (Naabil et al. 2017). Flooding in Burkina Faso in 2018 killed 100,000 people and devastated 196 square miles of agricultural land, including the Tono irrigation zone, as a result of heavy rains caused by the discharge of water from the Bagre dam (Floodlist 2018; Almoradie 2020). The frequency of heavy rainstorms in West Africa, particularly in Ghana, is anticipated to rise as a result of climate change, resulting in more devastating floods (IPCC 2012; Andersen and Marshall 2013; Naabil et al. 2020). Flooding may become more intense and occur more frequently as a result of human-caused activities such

✉ Edward Naabil
naabil.edward@bolgatu.edu.gh

Kouakou Kouadio
kk.kouadio@yahoo.fr

Benjamin Lamptey
bllamptey@gmail.com

Thompson Annor
tommykak@yahoo.com

Ifeanyi Chukwudi Achugbu
ifeanyi.chukwudi@fuoye.edu.ng

¹ Department of Agricultural Engineering, Bolgatanga Technical University, Bolgatanga, Upper East Region, Ghana

² Laboratoire des Sciences de la Matière, de l'Environnement et de l'Energie Solaire, Université Felix Houphout-Boigny, Abidjan, Côte d'Ivoire

³ School of Earth & Environment, University of Leeds, Leeds, UK

⁴ Faculty of Physical Sciences, Physics, Kwame Nkrumah University of Science and Technology, Kumasi, Ashanti, Ghana

⁵ Water Resources Management and Agrometeorology, Federal University Oye-Ekiti, Oye, Nigeria

as land-use changes linked to increased urbanization (Chang and Franczyk 2008; Delgado et al. 2010; Kalantari et al. 2014). Preparation time for disaster response teams and the deployment of flood risk reduction measures are aided by early warning systems (Givati et al. 2016). To create plans for long-term sustainability and adaptation, water resource managers can make use of drought estimates. It is critical to have accurate estimates of precipitation amounts and distribution in order to make accurate flood predictions (Younis et al. 2008; Shih et al. 2014). It is possible to predict flood occurrences using data from rain gauges as well as data from radar, remote sensing, and numerical climate models (Givati et al. 2016). Global weather forecast models are used to generate coarse, low-resolution precipitation forecasts. They are unable to capture the sensitivity and complexity of complex, severe precipitation systems resulting from land-surface heterogeneity, mesoscale orography, and land–water contrasts (Fiori et al. 2014). In West Africa's semi-humid Sudanian climate, rainfall is highly controlled by mesoscale convective storms (MCS). Nearly half of Ghana's annual rainfall comes from monsoonal rains (Achempong 1982; Fink et al. 2006). Rainfall has been caused by orographic forces on Nigeria's Jos Plateau (Omotosho 1985). These precipitation-induced factors are diverse in West Africa. There are too many spatial and temporal inconsistencies in the coarse global climate models to be useful. Heinzeller et al. (2014), applied the Weather Research Forecasting (WRF) model to produce high-resolution rainfall for West Africa to address these limitations. High-resolution precipitation estimates for Ghana were developed by Naabil et al. (2017) using a physical parameterization that followed the physics options (large dams). They demonstrated that utilizing high-resolution grids of 5 km, the WRF model could reasonably estimate precipitation amounts and distributions.

Hydrological and atmospheric models can be used in conjunction or separately to compute temperature, precipitation, and stream flow in recent studies (Yucel et al. 2015; Arnault et al. 2015; Gochis et al. 2015; Givati et al. 2016; Naabil et al. 2017). In some cases, the uncertainty related with the spatial distribution of high-intensity precipitation can be minimized by integrating high-resolution atmospheric models with high-resolution hydrological models (Yucel et al. 2015). It has been shown that forecasts of rainfall and temperature, runoff, streamflow, and floods can be reasonably reproduced when fine-scale, coupled hydro-meteorological models with effective grid resolution of a small number of kilometers (Gochis et al. 2015; Arnault et al. 2015; Senatore et al. 2015; Givati et al. 2016; Naabil et al. 2017).

Senatore et al. 2015, Wagner et al. 2016, and Givati et al. 2016 claim that coupled atmospheric–hydrological models outperform uncoupled models for some meteorological variables. According to their findings, convective storms are better forecasted using a fully coupled model.

Using a fully coupled model to estimate rainfall and temperature over West Africa, specifically the Tono basin, this study improved on previous findings. This was also the case because of the incorporation of the Tono dam in the model. This is the first study to examine the dam's effect on modeling the local climate in the basin by placing the geographic data (such as the dam's location) in the model setup. Its goal is to provide answers to the following queries:

1. Is a coupled hydro-meteorological model better at simulating rainfall and temperature than a standalone model?
2. Is it possible to increase the accuracy of rainfall and temperature estimates based on the choice of the forcing data?

For the creation of meteorological variables, both WRF (standalone) and coupled WRF-Hydro were employed with identical input data and model physical parameterization. Described in detail in “Data and methods” and “Results and discussion” sections, is the study area and the study approach respectively. “Conclusions” section is the presentation of the results and discussion, while Sect. 5 concludes the discussion with suggestions.

Data and methods

The study area

The WRF model's two stacked grids depict a map of the West African (WA) region, which serves as the study's domain (Fig. 1a). Ghana's northern and Burkina Faso's southern regions are connected by the Tono basin, which is located in the middle of the nested area (Fig. 1b). Located in West Africa, Ghana has a complex climate and hydrological regime that varies greatly from year to year. It is the movement and interaction of two air masses that affects the temperature, rainfall, and humidity (Achempong 1982; Gordon 2006). The rainy seasons are controlled by the annual oscillation of the Intertropical Convergence Zone (ITCZ) between the northern and southern tropics. Humid Atlantic air is brought to Europe by south-westerly winds blowing south of the ITCZ. As a result of these winds, hot, dusty air from the Sahara Desert is being blown north of the ITCZ. This study focuses on the Tono basin in Ghana's northern part, which lies between latitudes 10° and 11°. May–November is the ITCZ's northernmost point and the primary wind is south-westerly; December–March is the 'Harmattan' wind's northernmost point and the primary wind is north-easterly.

Tono basin has a catchment area of about 650 km². The basin also has an irrigation system with a dam that spans 18.6 square miles and is 4 km long. The area receives about 950 mm fewer rains per year than the

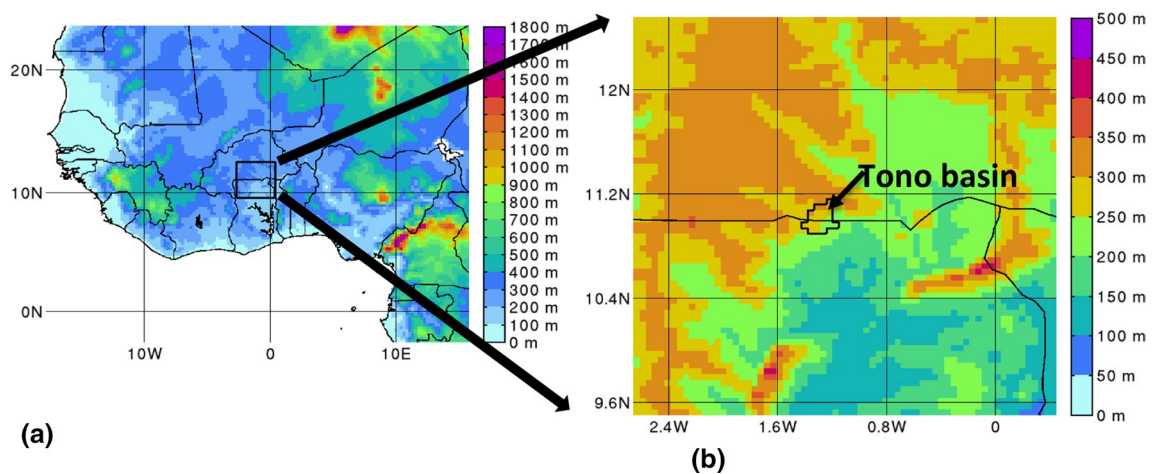


Fig. 1 Model domain and elevation. **a** The parent domain (25 km) with the imbricated nested domain (5 km) delimited by the back box. **b** A zoom on nested and high-resolution domain with the basin location

national average in Ghana. For its high temperatures and dryness, the region has been called one of Ghana's most arid areas. The highest monthly mean temperature (about 33 °C) is recorded in the months of March, April, and May (MAM), while the lowest monthly mean temperature (about DJF) is recorded in December, January, and February (26.5 °C).

The streams and rivers that empty into the basins are a reflection of the country's rainfall patterns. The Tono dam is fed by two major, unmeasured streams (Songoguba and Gaabuga).

The area's vegetation, which is the longest vegetation zone in Ghana, consists mainly of interior forest savannah (Anim-Gyampo et al. 2013). The basin's major function is to provide agricultural irrigation.

Data

Different gridded data sets were used depending on their temporal and spatial characteristics. The Tropical Rainfall Measuring Mission data were used to evaluate the model's precipitation performance (TRMM). The CRU's (Climate Research Unit) data collection for Africa, version TS3.0, is used to calculate the simulated temperature (Mitchell and Jones 2005). Interpolating CRU temperature from a 50-km resolution to a 5-km grid using Sibson's (1981) Natural Neighbor interpolation. The National Center for Atmospheric Research (NCAR) has been using this technique for a long time now (Hofstra et al. 2008). This allows for a comparison with the output of the Regional Climate Model (RCM) at the same grid resolution to evaluate the performance of the model.

Methodology

Atmospheric model (WRF) setup

The effect of model data selection on the success of model simulations in reproducing rainfall and temperature data was studied using two model data. Separate runs of the WRF model were driven by data from the 0.8° ERA-Interim reanalysis and the 0.5° ECHAM6 model. The model consists of two overlapping domains. There are 160 × 130 grid points of 25 km cell size in the domain d01 (parent domain), which encompasses the West African region from – 19 W to 17 E and – 1.8 S to 22 N (Fig. 1a). With a 5 km resolution and 111 × 111 grid points, the d02 (inner domain) covers the area from – 3 W to 1.5 E and 8 S to 13 N. The inner domain is intended to improve the resolution of convective and mesoscale characteristics in Ghana's northern half and Burkina Faso's southern half (Naabil et al. 2017; Kouadio and et al. 2020) (see Fig. 1b). The Tono basin is located in this inner sphere (Fig. 1b). The model resolution and physical parameterizations were determined based on prior investigations in the West African region by Heinzeller et al. (2014) and Naabil et al. (2017). Physical parameterizations used in their studies provide a more realistic assessment of rainfall and temperature distribution over West Africa at 12 km horizontal resolution for the period 1980–2010. These parameterizations were used in Naabil et al.'s (2017) investigations, which verified comparable results achieved by Heinzeller et al. (2014). As shown in Table 1, the physical parameterizations they chose was used in this study. To avoid cumulus activity being resolved, the nested domain's cumulus scheme was turned off because its spatial resolution was on the convective allowing scale (between 3 and 5 km). With a model

Table 1 Parameters defining the channel characteristics

Channel	Parameters			
StreamOrder				
10,1	'Bw	HLINK	ChSSlp	MannN'
1	5.	0.02	2.0	1.5
2	10.	0.02	1.0	1.4
3	20.	0.02	0.5	1.3
4	30.	0.03	0.18	1.2
5	40.	0.03	0.05	0.55
6	60.	0.03	0.05	0.3
7	60.	0.03	0.05	0.25
8	60.	0.10	0.05	0.1
9	60.	0.30	0.05	0.03

top pressure of 20 hPa, the boundary layer with 35 vertical levels. With the Noah LSM, hydrological processes in the column are taken into account in fully integrated WRF/WRF-Hydro simulations (i.e., through fall, soil infiltration, vertical soil water movement, evapotranspiration, and accumulation of surface and underground runoff). There is a lot of evidence that configuration setting is highly influenced by the variable of interest, study region focus and verification techniques as well as reference data sets utilized (Sylla et al. 2013; Klein et al. 2015; Naabil et al. 2017).

Hydrological model (WRF-Hydro) setup

National Center for Atmospheric Research (NCAR) developed WRF-Hydro and integrated it with the WRF model to see if the combined model could better reflect observed climate variables than the standalone model. The WRF-Hydro model is a state-of-the-art hydrological model capable of accounting for the spatial distribution of meteorological and physical input factors (Gochis et al. 2013). Numerous hydrological parameters can be connected to atmospheric and other Earth system modeling systems using the model's supplemental suite (Givati et al. 2016). Earth's terrestrial hydrologic courses, which include surface, subsurface, and channel water distribution, are to be better represented by a new suite (Gochis et al. 2013). A wide range of terrestrial hydrologic routing physics are included in the various model versions (WRF-Hydro V3.0 was used). The surface and subsurface flow models utilized in this study were entirely distributed, three-dimensional, and variable saturation. The Noah Land Surface Model's one-dimensional coupling of topography routing channel and basin routing functions enables for more complicated land-surface states and fluxes to be taken into account (Gochis et al. 2013; Givati et al. 2016). It is a more accurate representation of terrestrial hydrologic processes as compared to the Noah Land Surface model, which uses

simplified vertical column models. Water movement into channels is estimated in the WRF-Hydro model by allocating the quantity of water that infiltrates into the soil column and a proportion that flows horizontally through the overland flow (Gochis et al. 2013).

The surface properties affect both the velocity of water and where it goes, as well as its duration. Because water takes longer to reach the channels when the surface is rough, there is a greater chance that it will seep into the soil before reaching the channel components when the channel surface is smooth (Givati et al. 2016). The model's roughness parameter (REFKDT) is responsible both streamflow time and volume. The default roughness parameter values were reported by Vieux and Moreda (2003). The model's stream order and channel routing parameters influence the stream order values (see Table 1). Due to the domain's stream order, WRF-Hydro default Manning roughness coefficient values are applied to channel pixels. The transition of channels from lower to higher gradient reaches with coarser material to low-gradient, sedimentary reaches, and the Manning roughness coefficient falls as the stream flow approaches the basin outlet (Givati et al. 2016). The WRF-Hydro routing modules are executed to the inner domain with the coupled model approach, although it can be executed to the routing components of the coarse domain. We did not employ this strategy because it would have required a lot of time and computing power to perform. This setup was used created in previous studies of Naabil et al. (2017) which showed a good capability of the model in reproducing observed streamflows over the Tono basin. Hence, this study applied this setup in coupling it with the atmospheric model to reproduce rainfall and temperature at the Tono basin.

WRF-Hydro calibration and validation process

This study relied on the calibration and validation outcome of the WRF-Hydro model for the Tono basin by Naabil et al. (2017), since the same study region, input data, and physics parametrization were used. The assessment of the strength of the coupled model to reproduce rainfall and temperature better than standalone model was carried out for the period 2000 to 2005.

A standalone WRF model and a fully coupled WRF/WRF-Hydro model system were run. ERA-Interim Reanalysis and the ECHAM6 forcing data were used in both simulations. The Taylor Diagram (Taylor 2001) was used to compare model outputs to observed rainfall and temperature data (Trim and CRU). Temporal patterns, temporal inaccuracies, and spatial variability are all described using the center-mean-square error (RMSE), correlation coefficients (R), and normalized standard deviation (σ). These are expressed using the following equations:

$$RMSE = \sqrt{\frac{\sum_{i=1}^N (P_i - O_i)^2}{N}}, \tag{1}$$

$$R = \frac{\sum (X_i - \bar{X})(Y_i - \bar{Y})}{\sqrt{\sum (X_i - \bar{X})^2 \sum (Y_i - \bar{Y})^2}}, \tag{2}$$

$$\sigma = \sqrt{\frac{\sum_{i=1}^N (X_i - \bar{X})^2}{N}}, \tag{3}$$

where X_i denotes the individual X measurements, Y_i represents the individual Y measurements, O_i denotes the i^{th} measured value, P_i is represents the i^{th} predicted value, N denotes the number of observations, and over bars stand for the mean of the measured or estimated parameters.

The dam area was added to the inner domain of the WRF model's static data (geo em.d02) and given the land-use category 17 designation (waterbody). This is to determine the dam's impact on the microclimate.

Results and discussion

Observed vs simulated precipitation

With TRMM data as a basis, coupled WRF-Hydro and WRF's abilities to reconstruct the Tono basin's annual cycle of average daily precipitation rates were compared (Fig. 2a, b). WRF and WRF-Hydro simulations mirror the overall pattern of the annual cycle of rainfall over the basin, which is forced by ERA-I and ECHAM6 model data. The WRF-Hydro and WRF simulations forced with ECHAM6

agreed with TRMM in displaying the peak in August, however, WRF simulations forced with ERA-I rather shows an early peak (in July). The results also shows that both models, WRF and WRF-Hydro over-estimated precipitation amounts. However, WRF-Hydro has a lower bias than WRF. While WRF driven by ERA-I has a one-month earlier peak, WRF driven by ECHAM6 is better at simulating the annual cycle of rainfall, in particular the date of peak rainfall. Regardless of the forcing data, the annual cycle of daily rainfall shows that the coupled model produces a superior estimate of rainfall than the uncoupled atmospheric model. Analysis of the WRF and WRF-Hydro models' ability to extract daily rainfall in the Tono basin is carried out using the Taylor diagram statistical technique (Fig. 3). This graph summarizes three statistical measurements (the Root Mean Square Error, the standard deviation, and the Pearson correlation coefficient). Therefore, a good simulation should

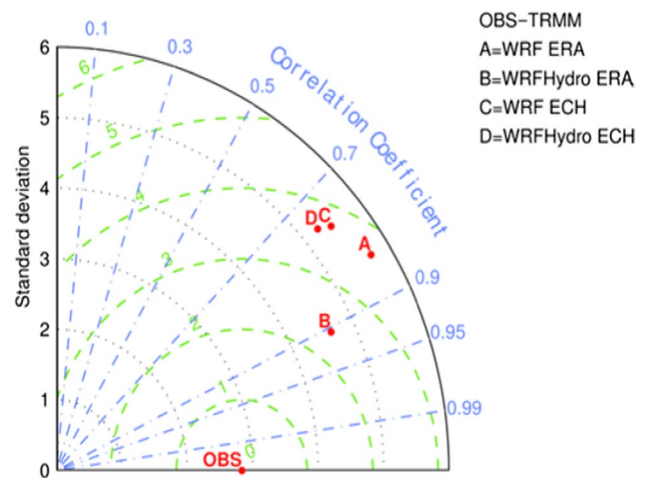


Fig. 3 Inter-comparison of WRF standalone and WRF-Hydro precipitation with respect to TRMM

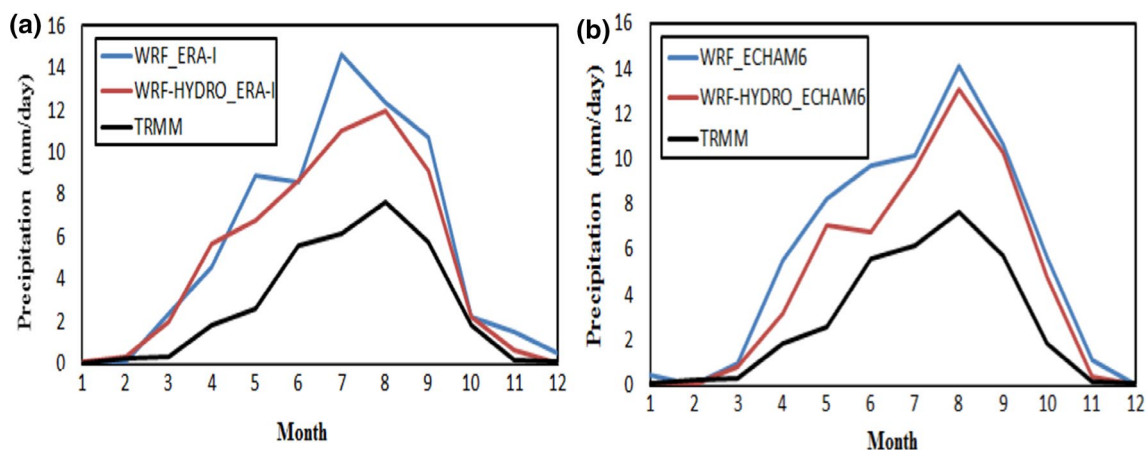


Fig. 2 Precipitation plot at daily scale in months for the period 2000–2005 using a ERA-I and b ECHAM6 data sets

have a correlation coefficient of a high value, low RSME, and the correct standard deviation. When plotting x-axis data, the "OBS" portion of the graph will be closest to the generated patterns. The RMSE and correlation of these models will be low. This study uses TRMM data as a baseline. WRF and WRF/WRF-Hydro runs with ERA-I for the Tono basin produce high patterns (correlation) of 0.8 and 0.91, respectively. The WRF/WRF-Hydro RMSE is approximately 2.4 mm/day, as shown by the green outlines, while the WRF RMSE is 3.7 mm/day. The temporal variability (standard deviation) of the simulated pattern is proportional to the radial distribution away from the source of that variability. According to the black arc, the WRF/WRF-Hydro simulated rainfall has standard deviation values of around 4.75 mm/day and 5.8 mm/day for WRF, which are higher than the observed standard deviation (2.9 mm/day) of rainfall. For ECHAM6 data, the pattern of correlation coefficient for WRF and WRF-Hydro models is 0.75, and the RMSE is 3.8 mm/day (Fig. 3). According to the data, the standard deviation (2.9 mm/day) is larger than the expected standard deviation (5.4 mm/day for WRF and 5.2 mm/day for WRF/WRF-Hydro). When it comes to retrieving the peak of the rainy season, simulations forced with ECHAM6 provide a good estimate of the annual cycle of rainfall, however, not superior when compared to runs forced with ERA-I. This could indicate that on a daily scale, the information provided by the forcing data appears to override the hydrologic feature provided by WRF-Hydro. ERA-I forcing data has shown

to provide a more improved precipitation estimation compared to ECHAM6 with both models (WRF and WRF/WRF-Hydro). It is clear in this case that the choice of a forcing data influence the performance of the models in reproducing precipitation. The ERA-Interim reanalysis has been shown in several studies to reasonable simulate regional climate and precipitation in the region (e.g., Heinzeller et al. 2014; Klein et al. 2015; Arnault et al. 2015; Annor et al. 2018).

The seasonal analysis in the basin focuses on the wet season (JJA, SON). As seen in Figs. 4 and 5, both WRF and WRF/WRF-Hydro show positive bias in rainfall. The seasonal (JJA and SON) assessment of both models driven by ERA-I indicates that the WRF model over-estimated precipitation at the basin compared to WRF/WRF-Hydro (Fig. 4). When ECHAM6 is applied to both models, the same results are seen (Fig. 5). Both models driven by ECHAM6 over-estimate precipitation compared to both models driven by ERA-I. Soil moisture dynamics and related effects could explain the significant biases of these models, which could result in major differences in the geographical distribution of rainfall based on the latitudinal positioning of irrigation (Marcella and Eltahir 2013). Irrigation water's latitudinal location and seasonal fluctuations appear to have a large impact on the rainfall distribution's response to irrigation. Precipitation forecasts from both models are nevertheless subject to uncertainty, even though WRF/WRF-Hydro output data show better accuracy than WRF output data for the Tono basin. This could be owing to the capacity of a fully

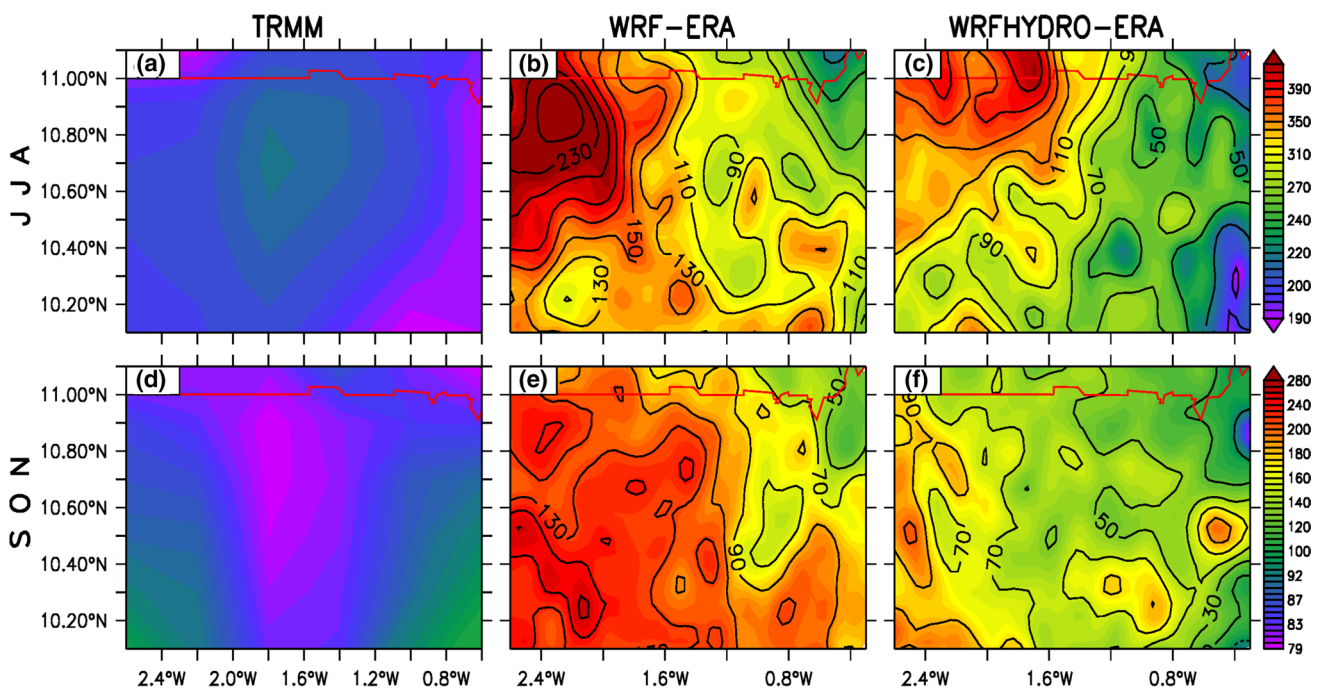


Fig. 4 Seasonal (SON and JJA) spatial precipitation maps over the Tono basin for the period 2000–2005 using ERA-I forcing data for WRF standalone and WRF-Hydro simulations

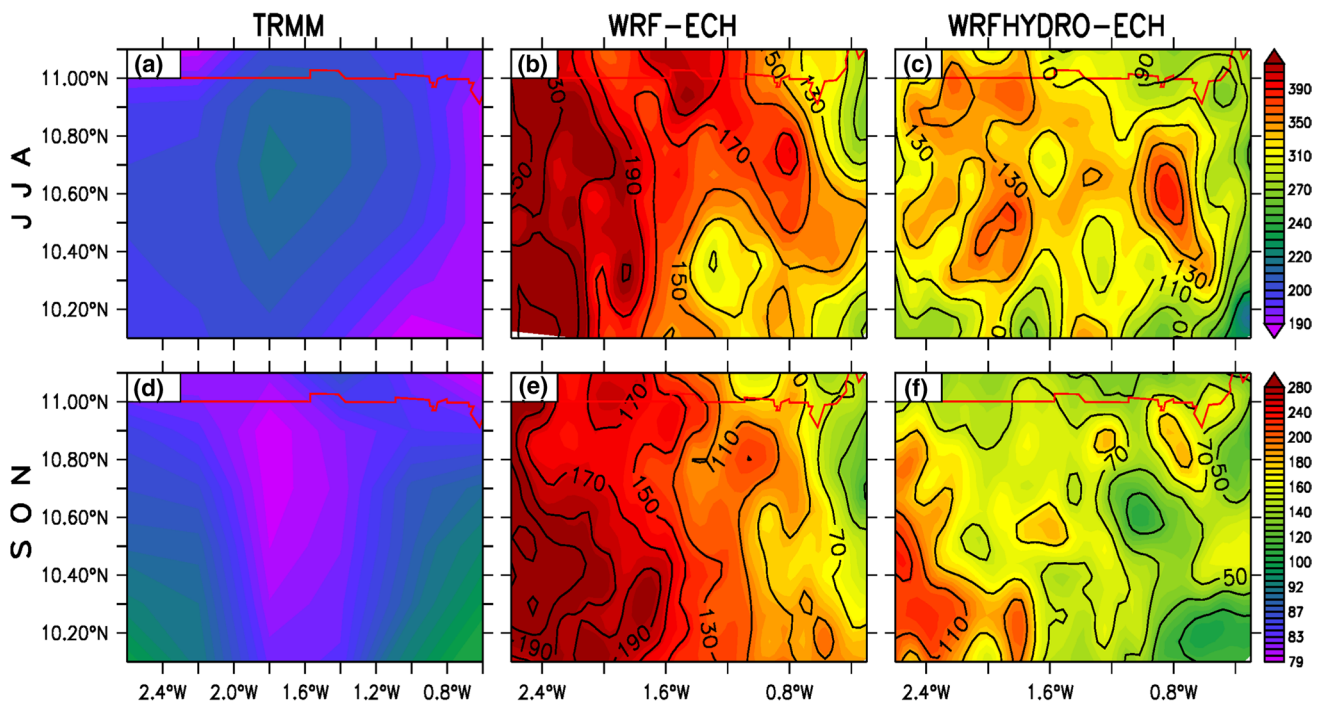


Fig. 5 Seasonal (SON and JJA) spatial precipitation maps over the Tono basin for the period 2000–2005 using ECHAM6 forcing data for WRF standalone and WRF-Hydro simulations

integrated land–atmosphere modeling system’s ability to simulate the complete regional water cycle in an integrated, mass- and energy-efficient manner (Senatore et al. 2015). There is evidence to suggest that coupled model simulations outperform uncoupled models over timescales longer than the average amount of daily precipitation (Jiang et al. 2009; Senatore et al. 2015; Givati et al. 2016). Using a groundwater model in conjunction with an atmospheric model, Jiang et al. (2009), demonstrated how the right energy flux and soil moisture signal from the land surface are critical in

predicting rainfall across the central United States. Coupling can increase precipitation reproducibility, as shown in this study.

Observed vs simulated temperature

For the Tono basin, monthly mean temperatures are shown in Fig. 6 using WRF and WRF/WRF-Hydro models with ERA-I and ECHAM6 forcing data. Both runs (WRF and WRF/WRF-Hydro) produce a good estimate of the annual

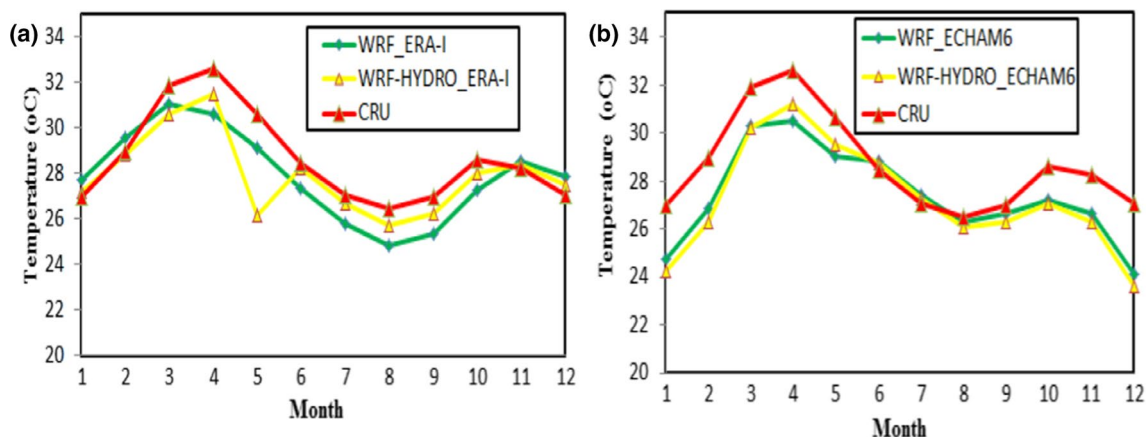


Fig. 6 Annual cycle of the monthly mean temperature over the period 2000–2005 using ERA-I **a** and ECHAM6 **b** data sets

monthly mean temperature when compared to observations (CRU). When compared to actual measurements at the basin's grid point, WRF/WRF-Hydro provides a more accurate temperature prediction than the standalone WRF (Fig. 6). It's possible that this has anything to do with the idea of coupling land–atmosphere systems in order to better depict temperature variability. Zeng et al. (2003), demonstrated that land-surface temperature and moisture heterogeneities have a considerable impact on sensible (H) and latent (LE) fluxes due to the coupling of atmospheric and land-surface processes. This is also reflected in estimates of evaporation and patterns of precipitation. Dry-season temperatures are over-estimated by the WRF and WRF/WRF-Hydro models (Fig. 6). A comparable study by Zeng et al. (2003), found that enhanced soil moisture fluxes during this period may have cooled the near-surface and influenced land-surface temperatures. Figure 7 shows the statistical inter-comparison of WRF and WRF/WRF-Hydro with CRU observation temperature over the Tono Basin using the Taylor diagram. For example, WRF/WRF-Hydro has a correlation of around 0.94 and an error margin of 0.6 °C when driven by the ERA-I. Compared to the measured temperature, the computed temperature has a lower standard deviation (1.8 °C). WRF driven with ERA-I has a correlation coefficient of about 0.87, while the RMSE and standard deviation are about 1.2 °C and 2.1 °C, respectively. This 2.1 °C standard deviation is equivalent to the observed temperature standard deviation (2.2 °C), implying that the pattern of changes in the simulated temperature from WRF forced with ERA-I is the same as observed data. There is an almost identical correlation (0.78) between WRF and WRF/WRF-Hydro driven by ECHAM6 with RMSE of 1.4 °C. While the simulated temperature standard deviation (2.0 °C) in WRF forced with ECHAM6 appears to be equal to the observed (2.2 °C) with CRU data, the one displayed by

WRF/WRF-Hydro forced with ECHAM6 has higher values (i.e., 2.6 °C). The WRF and WRF/WRF-Hydro, driven with ECHAM6, are projected to be farther to the observation than the WRF and WRF/WRF-Hydro, forced with ERA-I, based on RMSE and correlation coefficient patterns.

Figures 8 and 9 show the seasonal temperature bias maps, which reveal that both models underestimate temperature when compared to the observed data. WRF/WRF-Hydro forced with ERA-I produces a negative bias when compared to WRF forced with ERA-I in the dry season, according to a seasonal analysis using DJF season data. WRF/WRF-Hydro's negative bias was smaller than WRF's during the MAM season (Fig. 8). In both models that were forced with ECHAM6, WRF/WRF-Hydro did not add any value. Instead, it introduces more biases. When forced with ERA-I, WRF/WRF-Hydro has done better at modeling temperature, particularly at the basin. Zabel and Mauser (2013) discovered that simulations of a coupled atmospheric–hydrologic model improved the near-surface temperature. These new findings corroborate those of Zabel and Mauser (2013). As with rainfall estimates, WRF/WRF-Hydro forced with ECHAM6 model data did not produce satisfactory results with temperature estimation. Heinzeller et al.'s (2014) optimum physics settings for WRF across West Africa are also expected to influence the model's performance in terms of precipitation and temperature estimations.

Conclusions

Atmospheric–hydrological models were used to estimate precipitation and temperature in this investigation. It differs from previous studies by Naabil et al. (2017), which focused on the ability of WRF-Hydro to recreate hydrological variables for the assessment of long-term water resource sustainability.

When it came to precipitation, the models used in the study, WRF and WRF/WRF-Hydro, performed comparably well. Precipitation estimation was enhanced more by WRF/WRF-Hydro than by WRF. The WRF/WRF-Hydro forced with ERA-I beat the other model when tested with two sets of data (ERA-I and ECAHM6).

The fully coupled model showed some improvements in precipitation estimations when assessed on an annual cycle and seasonally. Three separate studies (e.g., Butts et al. 2014, Senatore et al. 2015 and Givati et al. 2016) have found that coupled model simulations outperform uncoupled model simulations for a longer period of time than the daily accumulation of rainfall, and this is consistent with the findings of this study. Water cycle modeling that incorporates both atmospheric and hydrologic processes can save both mass and energy because of the enormous potential of coupled atmospheric–hydrologic modeling systems (Senatore

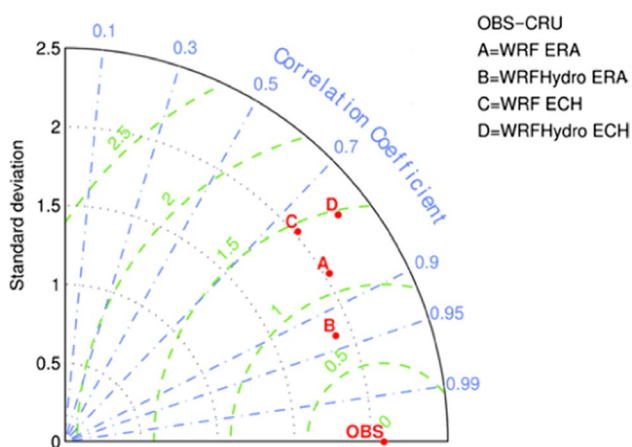


Fig. 7 Inter-comparison of WRF standalone and WRF-Hydro temperature with respect to CRU

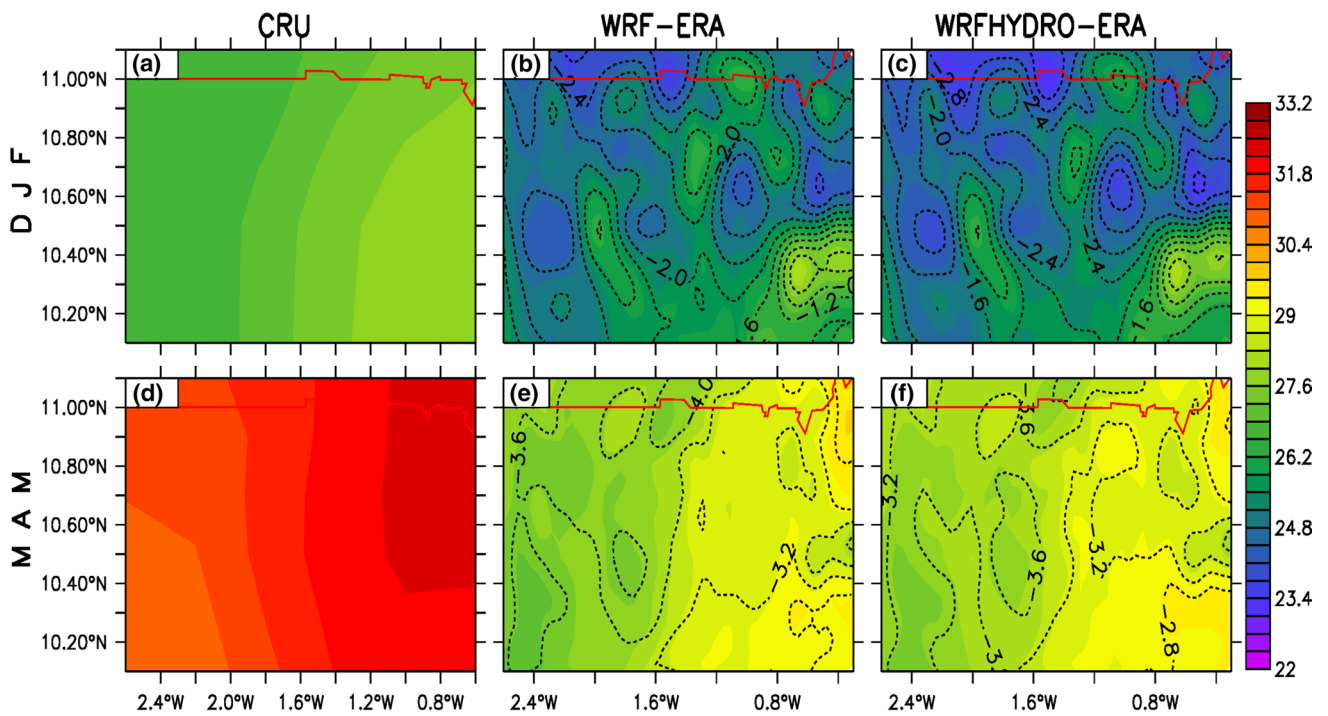


Fig. 8 Spatial temperature maps with bias values for the Tono basin for the period 2000–2005 using ERA-I forcing data for WRF standalone and WRF-Hydro simulations

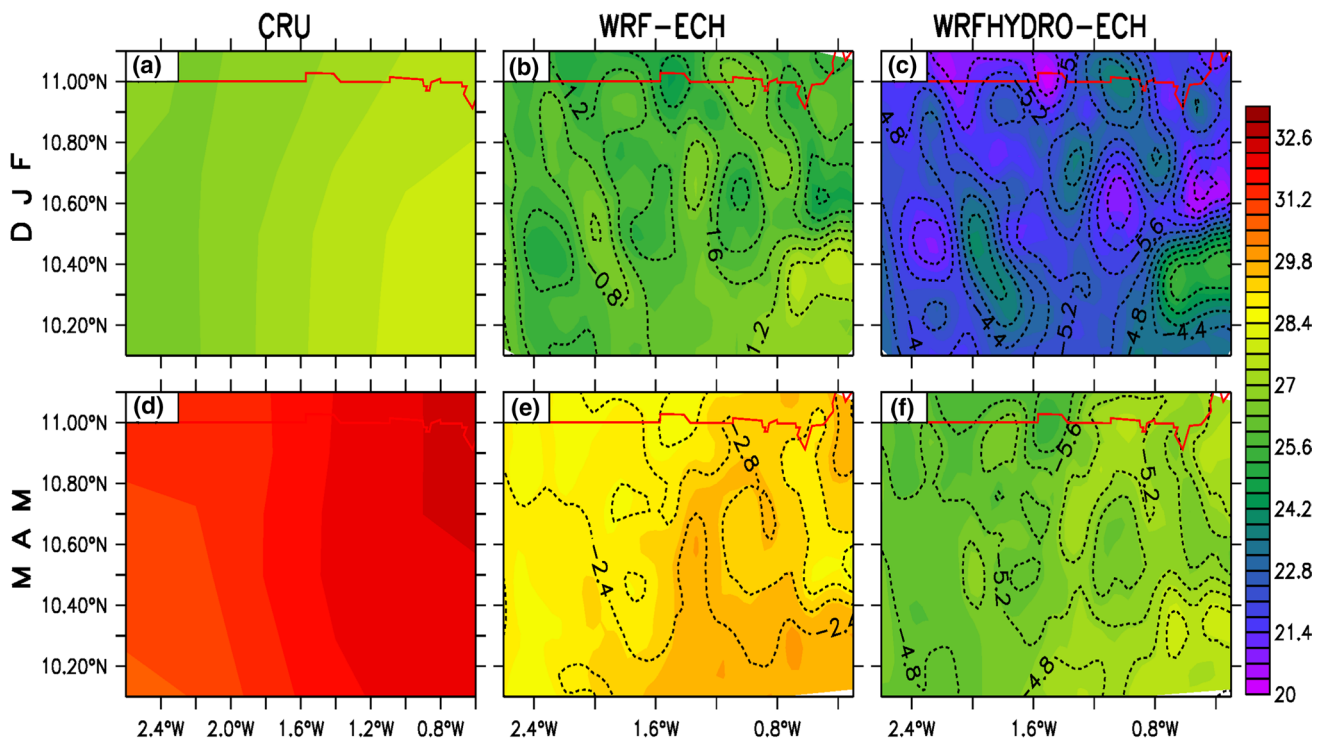


Fig. 9 Spatial temperature maps with bias values for the Tono basin for the period 2000–2005 using ECHAM6 forcing data for WRF standalone and WRF-Hydro simulations

et al. 2015). However, even though the coupled model was superior in terms of performance, the results revealed significant bias in the precipitation predictions, necessitating further research to discover the reasons of the bias and how it might be corrected. When it came to temperature estimation, neither model had any trouble reproducing the observed value. When compared with ERA-I, both models performed well when forced with the ECHAM6 model, which is a significant improvement.

A considerable benefit in precipitation and temperature forecasting has been proven by this investigation, supporting the notion that the coupled model is superior. Furthermore, the research shows that the ECHAM6 model data are insufficient for contemporary climate studies, particularly in West Africa.

Acknowledgements The research finance for this study was provided by the German Federal Ministry of Education and Research (BMBF) through the West African Science Service Center on Climate Change and Adapted Land Use (WASCAL). The computational facility was provided by the German Climate Computing Center (DKRZ).

Author contributions EN: Data curation (Lead), Formal analysis (Lead), Methodology (Lead), Validation (Lead), Writing—original draft (Lead), Writing—review and editing (Lead). KK: Formal analysis (Supporting), Methodology (Supporting), Writing—original draft (Supporting), Writing—review and editing (Supporting). BL: Formal analysis (Supporting), Methodology (Supporting), Writing—original draft (Supporting), Writing—review and editing (Supporting). TA: Formal analysis (Supporting), Writing—review and editing (Supporting). ICA: Writing—review and editing (Supporting).

Funding This research is the outcome of my PhD work which was financed by the German Federal Ministry of Education and Research (BMBF) through the West African Science Service Center on Climate Change and Adapted Land Use (WASCAL). However, the funding is no more available to pay for the cost of publication.

Data availability The data for this work can be sourced with permission from West African Science Service Center on Climate Change and Adapted Land Use (WASCAL) who are the repository of the data.

Declarations

Conflict of interest The authors declare that there is no conflict of interest with respect to this work.

References

- Achempong PK (1982) Rainfall anomaly along the coast of Ghana- its nature and causes. *Geogr Ann.* 64:199–211
- Almoradie A et al (2020) Current flood risk management practices in Ghana: gaps and opportunities for improving resilience. *J Flood Risk Manag.* <https://doi.org/10.1111/jfr3.12664>
- Andersen TK, Marshall SJ (2013) Floods in a changing climate. *Geogr Compass* 7:95–115
- Anim-Gyampo M, Kumi M, Zango MS (2013) Heavy metals concentrations in some selected fish species in Tono irrigation reservoir in Navrongo, Ghana. *J Environ Earth Sci* 3(1):2224–3216

- Annor T, Lamptey B, Wagner S, Oguntunde P, Arnault J, Heinzeller D, Kunstmann H (2018) High-resolution long-term WRF climate simulations over Volta Basin. Part 1: validation analysis for temperature and precipitation. *Theor and Appl Climatol* 144(3–4):829–849
- Arnault J, Wagner S, Rummeler T, Fersch B, Blieffernicht J, Andresen S, Kunstmann H (2015) Role of runoff-infiltration partitioning and additionally resolved overland flow on land-atmosphere feedbacks: a case study with the WRF-Hydro coupled modeling system for West Africa. *J Hydrometeorol.* <https://doi.org/10.1175/JHM-D-15-0089.1>
- Butts M, Drews M, Larsen MAD, Lerer S, Rasmussen S, Gross HJ, Overgaard J, Refsgaard JC, Christensen OB, Christensen JH (2014) Embedding complex hydrology in the regional climate system—dynamic coupling across different modelling domains. *Adv Water Resour* 74:166–184
- Chang H, Franczyk J (2008) Climate change, land-use change, and floods: toward an integrated assessment. *Geogr Compass* 2:1549–1579
- Delgado J, Llorens P, Nord G, Calder IR, Gallart F (2010) Modelling the hydrological response of a Mediterranean medium-sized headwater basin subject to land cover change: the Cardener River basin (NE Spain). *J Hydrol* 383:125–134
- Floodlist. (2018) Ghana—Dozens Killed by Flooding in Northern Regions. <http://floodlist.com/africa/ghanafloods-northern-regions-september-2018>
- Fiori E, Comellas A, Molini L, Reborá N, Siccardi F, Gochis DJ, Tanelli S, Parodi A (2014) Analysis and hindcast simulations of an extreme rainfall event in the Mediterranean area: the Genoa 2011 case. *Atmos Res* 138:13–29
- Fink AH, Vincent DG, Ermert V (2006) Rainfall types in the West African Sudanian Zone during the summer monsoon 2002. *Mon Weather Rev* 134:2143–2164
- Gordon C (2006) Background paper for the multi-stakeholder consultation process for dams development in Ghana. Volta Basin Research Project, University of Ghana. 67; <http://www.unep.org/dams/About.DDP/>. Accessed 22 Jun 2013.
- Gochis DJ, Yu W, Yates DN (2013) The WRF-hydro model technical description and user's guide, Version 1.0, NCAR Technical Document. NCAR, Boulder, Colo. 120; http://www.ral.ucar.edu/projects/wrf_hydro/
- Gochis D, Mc Creight J, Yu W, Dugger A, Sampson K, Yates D, Wood A, Clark M, Rasmussen R (2015) Multi-scale water cycle predictions using the community WRF-Hydro modeling system. NCAR, Boulder, CO USA
- Givati A, Gochis D, Rummeler T, Kunstmann H (2016) Comparing one-way and two-way coupled hydrometeorological forecasting systems for flood forecasting in the mediterranean region. *Hydrology.* <https://doi.org/10.3390/hydrology3020019>
- Hofstra N, Haylock M, Mark N, Phil J, Christoph F (2008) Comparison of six methods for the interpolation of daily European climate data. *J Geophys Res.* <https://doi.org/10.1029/2008JD010100>
- Heinzeller, D., Klein, C., Deing, D., Smiatek, G., Blieffernicht, J., Sylla, M.B., Kunstmann, H., (2014). The WASCAL regional climate simulations for West Africa: How to add value to existing climate projections. Held in June 24–26, 2014 in Boulder CO, U.S.A. www.mmm.ucar.edu/wrf/users/workshops/ws2015/posters/p63.pdf.
- IPCC (2012) Managing the risks of extreme events and disasters to advance climate change adaptation. In: Field CB, Barros V, Stocker TF, Qin D, Dokken DJ, Ebi KL et al (eds) A Special report of working groups I and II of the intergovernmental panel on climate change. Cambridge University Press, Cambridge, p 582
- Jiang X, Niu G-Y, Yang Z-L (2009) Impacts of vegetation and ground-water dynamics on warm season precipitation over the Central

- United States. *J Geophys Res Space Phys.* <https://doi.org/10.1029/2008JD010756>
- Kalantari Z, Lyon SW, Folkesson L, French HK, Stolte J, Jansson PE, Sassner M (2014) Quantifying the hydrological impact of simulated changes in land use on peak discharge in a small catchment. *Sci Total Environ* 466:741–754
- Klein C, Heinzler D, Bliefernicht J, Kunstmann H (2015) Variability of West Africa Monsoon patterns generated by a WRF multi-physics ensemble. *ClimDyn.* <https://doi.org/10.1007/s00382-015-2505-5>
- Kouadio K, Bastin S, Konare A, Ajayi VO (2020) Does convection-permitting simulate better rainfall distribution and extreme over Guinean coast and surroundings? *Clim Dyn* 55:153–174
- Larsen MAD, Refsgaard JC, Drews M, Butts MB, Jensen KH, Christensen JH, Christensen OB (2014) Results from a full coupling of the HIRHAM regional climate model and the MIKE SHE hydrological model for a Danish catchment. *Hydrol Earth Syst Sci* 18:4733–4749
- Marcella MP, Eltahir EAB (2014) Impact of potential large-scale irrigation on the West African monsoon and its dependence on location of irrigated area. *American Meteorological Society.* <https://doi.org/10.1175/JCLI-D-13-00290.1>
- Mitchell TD, Jones PD (2005) An improved method of constructing a database of monthly climate observations and associated high-resolution grids. *Int J Climatol: J Roy Meteorol Soc* 25(6):693–712
- Naabil E, Lamptey BL, Arnault J, Olufayo A, Kunstmann H (2017) Water resources management using the WRF-Hydro modeling system: case-study of the Tono dam in West Africa. *J Hydrol Reg Stud* 12:196–209
- Naabil E, Lamptey BL, Kouadio K, Annor T (2020) Climate change impact on water resources; the case of tono irrigation dam in Ghana. *Hydrology* 8(4):69–78. <https://doi.org/10.11648/j.hyd.20200804.12>
- Omotosho JB (1985) The separate contribution of line squalls, thunderstorms and the monsoon to the total rainfall in Nigeria. *J Climatol* 5:543–552
- Shih DS, Chen CH, Yeh GT (2014) Improving our understanding of flood forecasting using earlier hydro-meteorological intelligence. *J Hydrol.* 512:470–481
- Senatore A, Mendicino G, Gochis DJ, Yu W, Yates DN, Kunstmann H (2015) Fully coupled atmosphere-hydrology simulations for the central Mediterranean: Impact of enhanced hydrological parameterisation for short and long time scales. *J Adv Model Earth Syst* 7:1693–1715. <https://doi.org/10.1002/2015MS000510>
- Sibson R (1981) A brief description of natural neighbour interpolation. In: Barnett (ed) *Interpreting multivariate data.* John Wiley and Sons, Chichester, pp 21–36
- Sylla MB, Giorgi F, Pal JS, Gibba P, Kebe I, Nikiema M (2015) Projected changes in the annual cycle of high-intensity precipitation events over West Africa for the late twenty-first century. *J Clim* 28:6475–6488
- Sylla MB, Diallo I, Pal JS (2013) West African monsoon in state-of-the-science regional climate models, climate variability—regional and thematic patterns. In: Tarhule, Dr. Aonover (Ed.), *InTech.* <https://doi.org/10.5772/55140>. ISBN: 978-953-51-1187-0.
- Taylor KE (2001) Summarizing multiple aspects of model performance in a single diagram. *J Geophys Res.* 106:7183–7192
- Vieux BE, Moreda FG (2003) Ordered physics-based parameter adjustment of a distributed. *Calibration Watershed Models*, 267
- Wagner S, Fersch B, Yuan F, Yu Z, Kunstmann H (2016) Fully coupled atmospheric-hydrological modeling at regional and long-term scales: development, application, and analysis of WRF-HMS. *AGU Publ.* 52:4. <https://doi.org/10.1002/2015/WRF018185>
- Younis J, Anquetin S, Thielen J (2008) The benefit of high-resolution operational weather forecasts for flash flood warning. *Hydrol Earth Syst Sci* 12:1039–1051
- Yucel I, Onen A, Yilmaz KK, Gochis DJ (2015) Calibration and evaluation of a flood forecasting system; utility of numerical weather prediction model, data assimilation and satellite-based rainfall. *J Hydrol.* 523:49–66
- Zabel F, Mauser W (2013) 2-way coupling the hydrological land surface model PROMET with the regional climate model MM5. *Hydrol Earth Syst Sci* 17:1705–1714
- Zeng X-M, Zhao M, Su B-K, Tang J-P, Zheng Y-Q, Zhang Y-J, Chen J (2003) Effects of the land-surface heterogeneities in temperature and moisture from the “combined approach” on regional climate: a sensitivity study, *Global Planet. Change* 37:247–263

Publisher's Note Springer Nature remains neutral with regard to jurisdictional claims in published maps and institutional affiliations.

Springer Nature or its licensor (e.g. a society or other partner) holds exclusive rights to this article under a publishing agreement with the author(s) or other rightsholder(s); author self-archiving of the accepted manuscript version of this article is solely governed by the terms of such publishing agreement and applicable law.